

J. Electroanal. Chem., 350 (1993) 97–116
Elsevier Sequoia S.A., Lausanne
JEC 02543

Spectroscopic investigations of C₃ primary alcohols on platinum electrodes in acid solutions.

Part I. *n*-propanol

E. Pastor *, S. Wasmus and T. Iwasita

Institut für Physikalische Chemie der Universität Bonn, Wegelerstrasse 12, D-5300 Bonn (Germany)

M.C. Arévalo, S. González and A.J. Arvia **

Departamento de Química Física, Universidad de La Laguna, Tenerife (Spain)

(Received 15 September 1992; in revised form 22 October 1992)

Abstract

The electrochemical behavior of *n*-propanol (*n*-PrOH) on polycrystalline Pt in acid solutions was investigated using in situ Fourier transform infrared spectroscopy (FTIRS) and on line differential electrochemical mass spectrometry (DEMS). The main products of *n*-PrOH oxidation are CO₂, propanal and propionic acid. Different types of adsorbates with one, two or three C atoms were detected. Ethane and propane are produced from *n*-PrOH adsorbates during potential cycling in the H-atom potential region. An increase in the quantity of adsorbed CO was observed after hydrogenation of *n*-PrOH adsorbates.

INTRODUCTION

The interaction between organic molecules and metallic surfaces plays an important role in a number of electrochemical systems, ranging from electrocatalysis to metallic protection. This type of interaction may imply a direct adsorption of the organic molecules on the electrode or its electroadsorption either with or

* On leave from Departamento de Química Física, Universidad de La Laguna, Tenerife, Spain.

** Visiting Professor, INIFTA, Universidad Nacional de La Plata, Argentina.

without molecular splitting [1-3]. Among the adsorbates formed there are strongly adsorbed species which in many cases behave as catalyst poisons, and weakly adsorbed species which may act as true reaction intermediates [3-6]. Coadsorbate formation has also been observed [7,8].

In general, adsorption and electroadsorption phenomena on electrodes depend on several variables, such as the potential routine, the nature of the electrode and its previous treatment, and the electrolyte composition. Both the adsorption products and the structure of the adsorbates can change according to the experimental procedure [9-11].

Electrochemical kinetic data on the electro-oxidation of alcohols obtained by application of standard electrochemical methods are reported in the literature [5,12-13]. However, these results have intrinsic limitations for the identification of reaction products as well as for the determination of the corresponding faradaic yields.

Progress in the electrochemical studies of alcohol reactions requires the application of new spectroscopic methods such as differential electrochemical mass spectrometry (DEMS) [14,15] and in situ Fourier transform IR spectroscopy (FTIRS) [16-18]. DEMS is the most appropriate method for detection of traces of volatile products formed at submonolayer levels during the electrochemical process, and FTIRS gives access to the nature of adsorbed species through the identification of characteristic group frequencies.

The present paper is the first of a series devoted to investigating C₃ primary alcohols, namely, *n*-propanol (*n*-PrOH), allyl alcohol (AA) and propargyl alcohol (PA) on Pt electrodes in acid solution, by applying spectroscopic methods.

The literature on stationary electrocatalytic reactions of unsaturated alcohols has been surveyed in ref. 3. The presence of different unsaturated bonds in these alcohols produces distinct electrochemical behavior, presumably caused by adsorbates whose nature depends on the applied potential [5,9,10,12].

The electrochemical behavior of *n*-PrOH has been extensively studied on different electrodes in aqueous solutions [5,10,13,19]. Different electro-oxidation mechanisms have been proposed, particularly on Pt [5,13,19]. A number of products have been detected for both *n*-PrOH electroreduction [20] and electro-oxidation on Pt [21]. From the *n*-PrOH electroadsorption and anodic stripping charges various adsorbate structures have been postulated [10,19]. Preliminary DEMS results [21] and recently published FTIR data [22] of *n*-PrOH on Pt electrodes, indicate the convenience of applying these techniques to clarify the mechanism of this complex reaction.

EXPERIMENTAL

All experiments were performed at room temperature applying the electrochemical flow cell technique [23,24]. The transfer of solutions from storage flasks to the cell was made through glass tubing under an inert atmosphere. Gases were passed through the system using a stainless steel pipeline.

Solutions were prepared with Millipore MilliQ* water and *n*-PrOH (Aldrich, spec-grade) in the 0.01 M–1 M concentration range, with either 0.05 M H₂SO₄ (p.a.) or 0.1 M HClO₄ (p.a.) as the base electrolyte. Solutions were deaerated with Ar (99.998%) or N₂ (99.999%).

DEMS experiments were performed by directly coupling the electrochemical cell to a quadrupole mass spectrometer (Balzers QMG 112). The arrangement allowed the detection of volatile species from the electrochemical reaction with a delay of ca. 0.2 s after the species were formed. The mass signals could be recorded almost simultaneously with the cyclic voltammogram.

A small (2 cm³) flow cell made of plexiglass was used. The working electrode (WE) consisted of a Pt deposit prepared from a Doduco Pt lacquer suspension (average particles size 1–5 μm) onto a porous Teflon membrane. This membrane constitutes the electrolyte/vacuum interface and allows the permeation of volatile substances into the mass spectrometer. The geometric area of the WE was 0.64 cm² and the real area ranged between 150–200 cm². A Pt wire served as the counter electrode, and a reversible hydrogen electrode (RHE) in the respective base solution was used as reference. The WE was activated through triangular potential cycling at 0.01 V/s between 0.05 V and 1.55 V in the base solution until a reproducible voltammogram and a potential-independent CO₂ mass signal were obtained. The results are displayed as mass signal cyclic voltammograms (MSCV).

The Fourier transform IR spectrometer was a Digilab FTS-40 provided with a mercury-cadmium telluride (MCT) detector. Parallel (p) or perpendicular (s) polarized IR light was obtained from a BaF₂ supported Al grid polarizer. Standard electrochemical equipment was used.

A glass cell (ca. 6 cm³) with a CaF₂ optical window was used [25]. The cell was provided with an inlet and an outlet for solutions, so that electrolyte exchange could be achieved without interrupting the potential control. The WE was a polycrystalline Pt disk (1 cm diameter) axially embedded in glass. It was polished mechanically to a mirror surface with diamond paste, then dipped into 0.1 M HNO₃ for about 30 min, and thoroughly rinsed with Millipore MilliQ* water with the application of ultrasound. The counter electrode was a flat Pt ring 0.5 cm high and 2.8 cm in diameter. The reference electrode was a reversible hydrogen electrode (RHE) in the base electrolyte, 0.5 M HClO₄ solution.

An initial electrode pre-treatment consisting of repetitive potential cycles at 0.1 V/s between 0.05 V and 1.55 V was applied, to desorb residual impurities. During this treatment the solution was frequently replaced by flushing with fresh base electrolyte.

RESULTS

DEMS—bulk n-PrOH reactions

MSCVs obtained during the electro-oxidation of *n*-PrOH in 0.05 M H₂SO₄ + 0.01 M *n*-PrOH (Fig. 1), exhibit several potential-dependent *m/z* ratios, where *m*

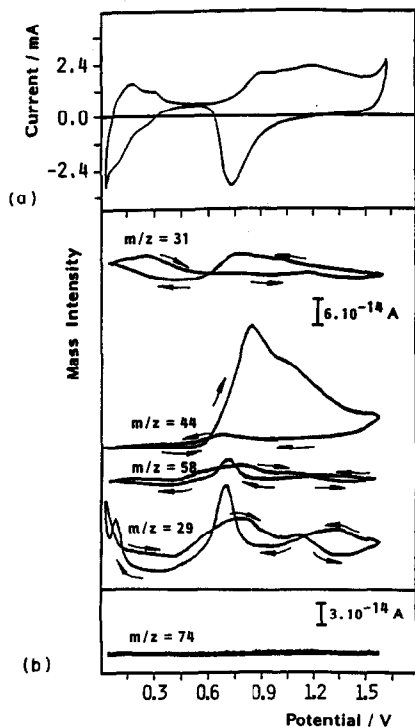


Fig. 1. (a) Cyclic voltammogram in 0.01 M *n*-PrOH + 0.05 M H₂SO₄ on porous Pt, $\nu = 0.01 \text{ V s}^{-1}$, and (b) mass signal cyclic voltammograms for $m/z = 31$ (propanol), $m/z = 44$ (CO₂), $m/z = 58$ (propanal), $m/z = 29$ (propanal, ethane and propane) and $m/z = 74$ (propionic acid).

is the mass and z is the charge of the fragment. The consumption of *n*-PrOH was followed through its main fragment (CH₂OH)⁺, $m/z = 31$ and the production of CO₂ through the signal for $m/z = 44$. The formation of propanal was observed through the signals for $m/z = 58$ and $m/z = 29$. The former corresponds to the radical cation of the propanal molecule M^{•+} and the latter is related to the (COH)⁺ fragment, which yields the main peak of the mass spectrum of propanal. In Fig. 1 the signal for $m/z = 74$ is also given. This mass corresponds to the radical cation M^{•+} of propionic acid. In 0.01 M *n*-PrOH we observed no changes in the ground signal with the applied potential. A small production of propionic acid was observed in 0.1 M *n*-PrOH solution at potentials above 1.00 V.

Below 0.25 V mass 29 reveals the contribution of at least two electroreduction products (Fig. 2). The signal for $m/z = 43$ corresponds to (CH₃-CH₂-CH₂)⁺, a fragment of propane; the signal for $m/z = 30$ is the M^{•+} of ethane overlapping a small contribution from propane; and the signal for $m/z = 15$ results from fragments of propane, ethane and negligible amounts of methane.

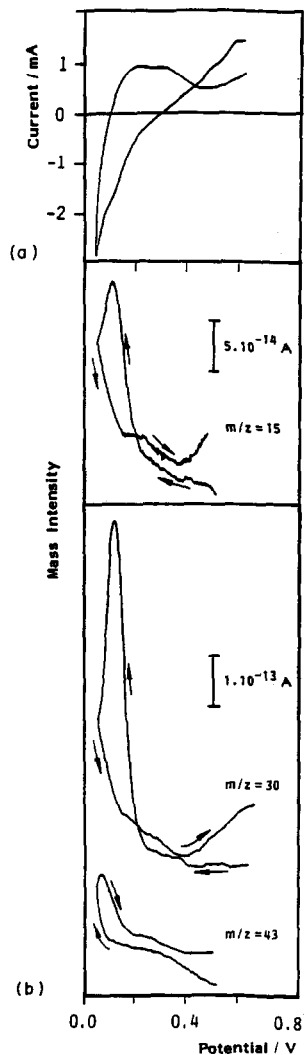


Fig. 2. (a) Cyclic voltammogram in 0.1 M PrOH+0.1 M HClO₄ at porous Pt, $v = 0.01 \text{ V s}^{-1}$ and (b) mass signal cyclic voltammograms for $m/z = 15$ (methane, ethane and propane), $m/z = 30$ (ethane) and $m/z = 43$ (propane). Only the Pt-H potential region is shown.

After taking into account the correction for the fragmentation in the MS (Table 1 [26]), the height of the ion current peaks was used to establish the relative yield ratio 30:10:1 for ethane:propane:methane. Gas chromatography results reported previously for the electroreduction of propanol [19] at 0.05 V indicate 19% ethane, 76% propane and 4% butane. The latter was not detected in the present work. This discrepancy could be as a result of differing experimental conditions.

TABLE 1

Relative intensity of MS signals of different fragments related to possible compounds of interest for the present work, taken from ref. 26

Compound	<i>m/z</i>								Total
	15	29	30	31	43	44	58	74	
Methane	815	—	—	—	—	—	—	—	1977
Ethane	33	223	269	—	—	—	—	—	2143
Propane	42	1000	18	—	279	336	—	—	3267
<i>n</i> -propanol	12	163	21	1000	33	7	12	—	2002
Propanal	—	1000	55	32	36	3	389	—	3307
Propionic acid	24	878	142	38	29	14	9	1000	6015

DEMS—adsorbed *n*-PrOH

The electrochemical behavior of adsorbates was investigated through MSCV without *n*-PrOH in the bulk of the solution. After electrode pretreatment, described above, the potential was set at the adsorption potential E_{ad} until a stable background current was reached. The solution was then exchanged with electrolyte containing *n*-PrOH under potential control. After adsorption, the solution was replaced by the base electrolyte while the potential was kept at E_{ad} . Finally, the CV and MSCV for the oxidation of the adsorbed residues were obtained.

Figure 3 shows typical results for different experimental conditions. CO_2 was the only oxidation product. We observed two current peaks, E_{p1} and E_{p2} during the positive scan. In the reverse scan of the MSCV a small peak E_{p3} is displayed at ca. 0.70 V. This peak has no visible counterpart in the corresponding CV owing to overlapping with the relatively high oxide reduction current. There is no doubt that peak E_{p3} results from the adsorbate and not from residual propanol. Exhaustive electrolyte replacement was performed to eliminate this possible source of error. However, the possibility that this peak results from some desorption products formed at the higher potentials, was ruled out by changing the electrolyte while the potential was held at 1.55 V. The peak remained even after this procedure.

For the complete electro-oxidation of *n*-PrOH adsorbates at least two oxidation cycles up to 1.55 V are required in both base electrolytes (Fig. 3(a)). Similar results could be obtained by holding the potential at 1.55 V for 15 min including the solution renewal.

Figure 3(b) shows CVs obtained at different adsorption potentials after cycling the potential four times in the H-region. E_{p1} shifts to lower potentials and the total oxidation charge decreases.

The oxidation peaks are better defined in the MSCV than in the CV. We therefore analysed the peak potential data from the MSCV and the charge data from the CV. The results are assembled in Table 2.

Examination of the data in Table 2 indicates that at a given adsorption potential the nature of the supporting electrolyte (H_2SO_4 or $HClO_4$) has a pronounced

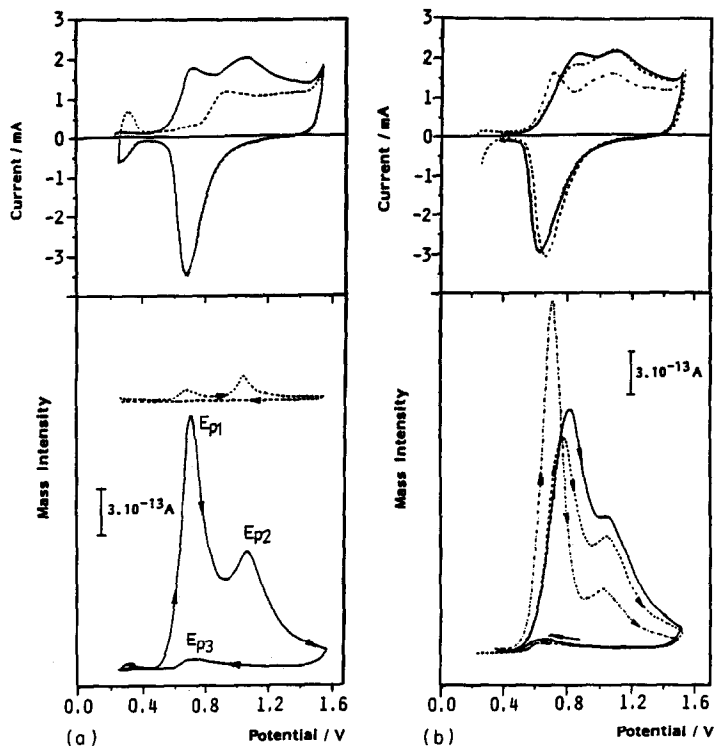


Fig. 3. Cyclic voltammogram of n -PrOH adsorbates and mass signal cyclic voltammogram for $m/z = 44$ (CO_2), $v = 0.01 \text{ V s}^{-1}$. (a) $E_{\text{ad}} = 0.22 \text{ V}$ in 0.1 M HClO_4 : (—) 1st cycle; (-----) 2nd cycle. (b) $0.05 \text{ M H}_2\text{SO}_4$: (—) $E_{\text{ad}} = 0.35 \text{ V}$, direct oxidation of the adsorbate; (-----) $E_{\text{ad}} = 0.22 \text{ V}$, direct oxidation of the adsorbate; (·-·-·) $E_{\text{ad}} = 0.35 \text{ V}$, oxidation after 4 cycles in the Pt-H potential region.

TABLE 2

E_{p1} , E_{p2} and E_{p3} potentials of the voltammetric anodic peaks related to the first electro-oxidation cycle of n -PrOH adsorbates formed on Pt at E_{ad} . N_{H} = number of cycles in the Pt-H potential region, q_{ox} = electro-oxidation charge of n -PrOH adsorbates. WE area = 175 cm^2

Base electrolyte	E_{ad}/V	N_{H}	E_{p1}/V	E_{p2}/V	E_{p3}/V	q_{ox}/mC
0.05 M H_2SO_4	0.35	4	0.73	1.05	0.67	58
	0.22	4	0.73	1.05	0.68	52
	0.35	20	0.73	1.05	0.68	57
	0.35	0	0.84	1.07	0.67	82
	0.22	0	0.81	1.08	0.68	82
0.1 M HClO_4	0.35	4	0.70	1.08	0.75	53
	0.35	0	0.77	1.08	0.74	81
	0.22	0	0.71	1.09	0.74	85

influence on E_{p1} and E_{p3} , while E_{p2} is much less affected. E_{p1} is more positive in H_2SO_4 than in $HClO_4$. Similarly H_2SO_4 retards the oxidation peak observed during the negative scan, i.e. E_{p3} appears at more positive potentials in $HClO_4$. Also, the threshold potential for *n*-PrOH adsorbate oxidation in $HClO_4$ is lower than in H_2SO_4 . These facts are probably related with the adsorption of bisulphate ions on Pt [27]. In general, the maximum degree of coverage with adsorbed anions is no more than ca. 0.1 [28]. Therefore, unless bisulphate can exert long range lateral forces, the observed effects on propanol adsorbate oxidation would be difficult to understand. Bisulphate adsorption on single crystal platinum electrodes has recently been described [29] as an arrangement of anions and water clusters, forming a kind of network, stabilized by hydrogen bonding. We suggest that this network is involved in the adsorbate stabilization. In particular, oxygen-containing adsorbed species (see below) could be fixed in this network by forming hydrogen bonds with bisulphate and water. This could explain the delayed electro-oxidations (E_{p1} and E_{p3}) observed in sulphuric acid.

The desorption products resulting from *n*-PrOH adsorbates subjected to cycling in the potential range of H-adatoms (Fig. 4) are propane ($m/z = 43$) and ethane ($m/z = 30$). In the first cycle of the CV run between 0.35 V and 0.05 V (Fig. 4(a)), we observed a cathodic current larger than the anodic one, due to the hydrogenation processes yielding the observed hydrocarbons. The MSCVs reveal that the largest production of ethane and propane takes place during the first CV and decays rapidly in the following cycles, approaching zero after the fourth cycle. The ratio of the mass intensities for ethane and propane from the first CV indicates that the production of ethane is ca. 3.5 times greater than that of propane. Approximately the same ratio results from *n*-PrOH bulk electroreduction. These results suggest that the amount of hydrogenated adsorbates with C-C bonds on the Pt surface is about three times larger than for adsorbates with intact C-C-C bonds.

FTIRS—spectra of soluble products

For the FTIR studies of soluble oxidation products we set the potential at 0.25 V in the base electrolyte, and then replaced the solution with the *n*-PrOH electrolyte. Spectra were then taken at selected potentials ranging from the initial potential (reference spectrum) to 1.50 V, by applying single potential steps.

From the values of R and R_0 , the reflectance at the selected and at the reference potential, respectively, the reflectance ratio R/R_0 was determined at each potential. Positive and negative bands are associated respectively with loss and gain of substances at the sample potential.

Figure 5 shows spectra at different potentials in the presence of bulk propanol. At 0.50 V the CO stretching bipolar band for linear adsorbed CO at 2041–2053 cm^{-1} , and the negative (gain) bands at 1640 and 1126 cm^{-1} corresponding to water and ClO_4^- ions, respectively, were observed. New positive (loss) and negative bands developed as the applied potential was increased positively.

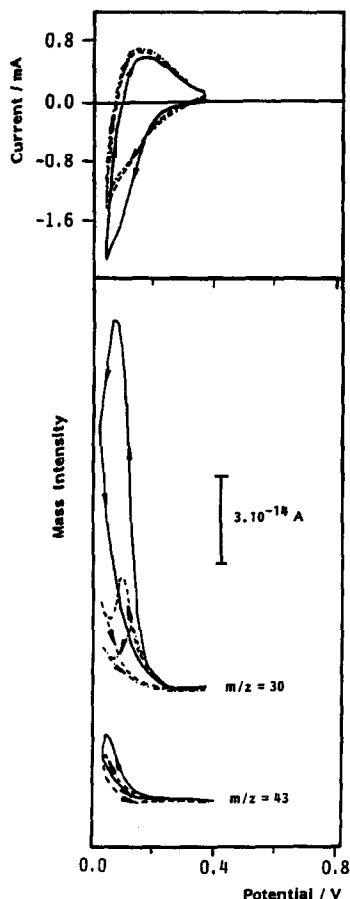


Fig. 4. (a) CVs during the electroreduction of *n*-PrOH adsorbates; (b) MSCVs for $m/z = 30$ (ethane) and $m/z = 43$ (propane) during continuous cycling between $E_{ad} = 0.35$ V and 0.05 V. $v = 0.01$ V s⁻¹, 0.05 M H₂SO₄. (—) 1st cycle, (-----) 2nd cycle, (·-·-·) 3rd cycle.

At 0.70 V, the CO₂ asymmetric stretching vibration band appears at 2343 cm⁻¹. The positive bands at 2971, 2941, 2886, 1045, 1004 and 960 cm⁻¹ are due to the loss of *n*-PrOH molecules as they become oxidized.

The C=O stretching band from a carbonyl group appears at 1713 cm⁻¹. This band can be related to the presence of propanal and/or propionic acid. However, other features at 1466, 1385 and 1226 cm⁻¹, which are clearly developed at 1.20 V, indicate the presence of propionic acid. For comparison, a transmission spectrum of the latter in an aqueous solution is shown in Fig. 6. It should be noted that the formation of propionic acid in the electro-oxidation of *n*-PrOH has been recently proposed from FTIRS data [22], although not definitely demonstrated because the relevant bands in the mentioned publication are masked by the background

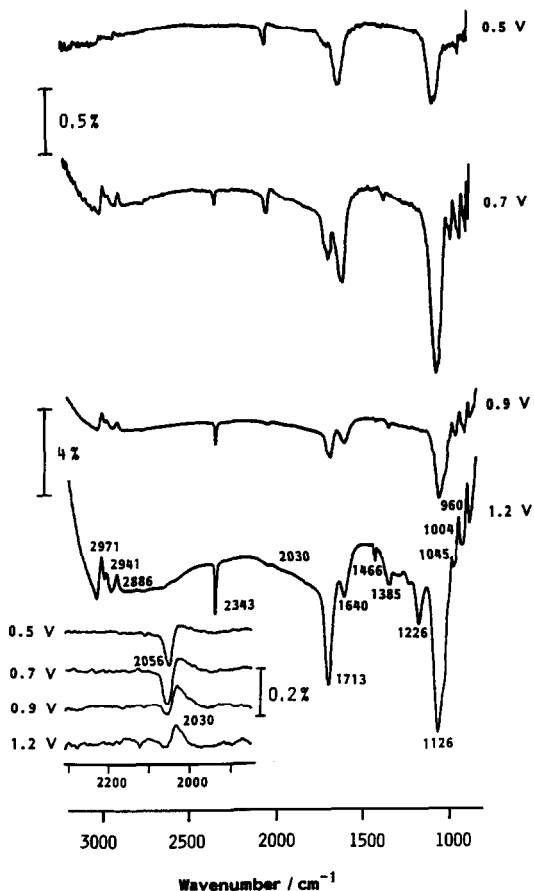


Fig. 5. FTIR reflectance spectra from polycrystalline Pt in 0.1 M *n*-PrOH+0.5 M HClO₄. All spectra (256 scans each, 8 cm⁻¹ resolution) are normalized to the reference spectrum collected at 0.25 V. Note that the scale for the spectra at 0.5 V and 0.7 V is 0.5%, and the scale for the spectra at 0.9 V and 1.2 V is 4%.

absorption of HSO₄⁻ ions from the base electrolyte. We obtained spectra with s-polarized light which confirmed that propionic acid is a solution product.

The bands relating to *n*-PrOH consumption and propionic acid formation can be considerably enhanced by increasing the *n*-PrOH concentration (Fig. 7). This is not, however, the case for the CO₂ band. Carbon dioxide is thus mainly produced from adsorbed species. Furthermore, in 1 M *n*-PrOH two weak bands at 2850 and 2757 cm⁻¹ are well defined and can be assigned to C-H stretching of species containing the aldehyde group. The apparent inconsistency between FTIRS data, showing the formation of both propanal and propionic acid, in contrast to DEMS,

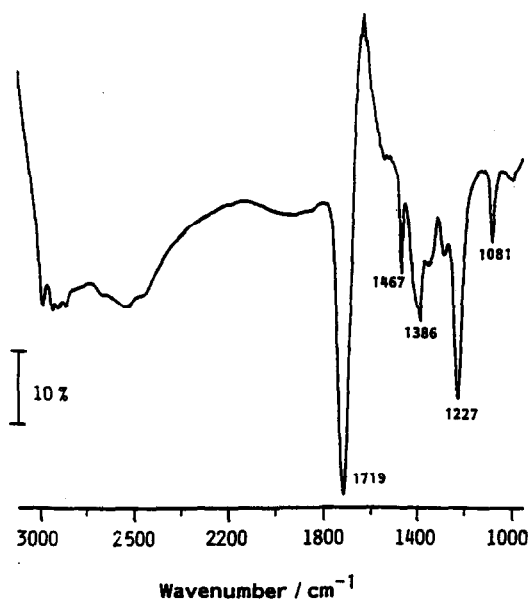


Fig. 6. Transmittance spectrum of 1 M propionic acid with a background spectrum of water.

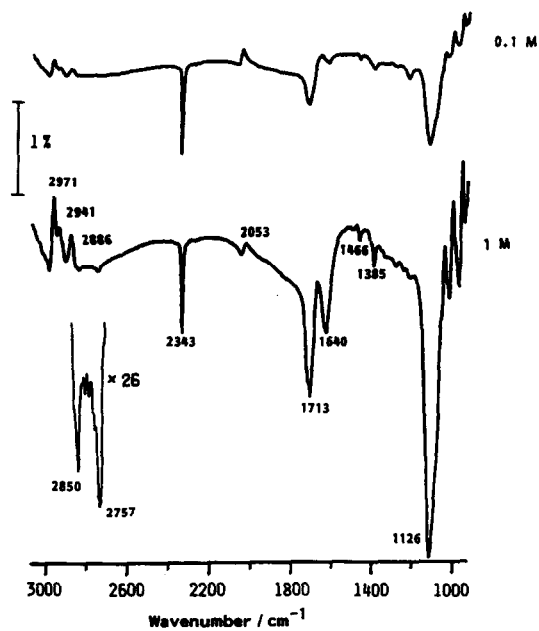


Fig. 7. Comparison of FTIR spectra (256 scans each, 8 cm^{-1}) for 0.1 M and 1 M *n*-PrOH in 0.5 M HClO_4 at 0.90 V. Reference spectrum taken at 0.25 V.

providing evidence for aldehyde formation only, can be attributed to experimental technique. Thus, taking into account the sequential reaction



and the difference in the volatility of propanal (b.p. 48.8°C) and propionic acid (b.p. 141°C), it is possible that propanal is pumped into the mass spectrometer before it can react to propionic acid. This would reduce the possibility of propionic acid detection through DEMS. In contrast, FTIRS shows that the diffusion of products out of the thin layer occurs rather slowly favouring the accumulation of propionic acid and its detection.

FTIRS—*n*-PrOH-adsorbed species

The nature of the strongly adsorbed species was investigated after adsorption and electrolyte exchange as described for DEMS. Propanol was adsorbed for 5 min at $E_{\text{ad}} = 0.35$ V, then the solution was exchanged with pure supporting electrolyte. Our potential program (see insert in Fig. 8), was directed towards the detection of absolute IR bands for adsorbed species. After taking the reference spectrum R_0 at the adsorption potential E_{ad} , a potential step to 1.55 V was applied in order to oxidize most of the adsorbate. The potential was then restored to E_{ad} and the

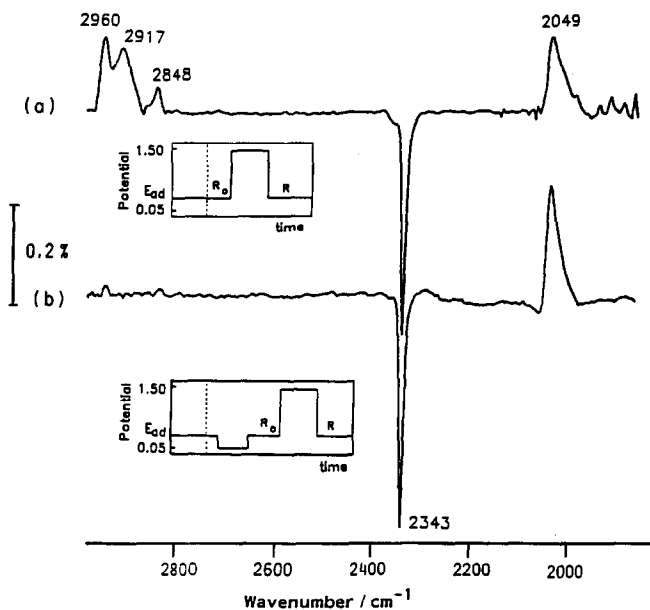


Fig. 8. Reflectance spectra (1000 scans each, 8 cm^{-1} resolution) for the strongly adsorbed species of *n*-PrOH. Potential programs were as indicated in the insert. $E_{\text{ad}} = 0.35$ V. The electrolyte exchange is indicated by the dotted lines. (a) Without reduction, (b) after reduction at 0.05 V.

sample spectrum (indicated in Fig. 8 as R) was taken. (Taking sample and reference spectra at the same potential diminishes the spectra distortion caused by potential-dependent changes.) In this way all species which become oxidized at 1.3 V, should present positive-going bands in the calculated R/R_0 spectrum.

In Fig. 8(a), together with the loss band for linear bonded CO at 2049 cm^{-1} , we observe other positive bands in the C–H stretch region at 2960, 2917 and 2848 cm^{-1} . These bands can be assigned to adsorbates containing CH_3 and CH_2 groups. According to the literature [30–32], the bands at 2960 cm^{-1} and 2917 cm^{-1} are due to the asymmetric stretching of CH_3 and CH_2 , respectively, and the band at 2848 cm^{-1} with a shoulder at 2869 cm^{-1} results from the overlapping of CH_2 and CH_3 symmetric stretching. It should be noted that these bands, which belong to adsorbed species, are shifted to lower frequencies than those for bulk propanol, shown in Figs. 5 and 7. For single CH_3 or CH_2 adsorbed species only the symmetric stretch should be IR active (surface selection rule). The fact that the spectra show the asymmetric as well as symmetric stretching for both groups, suggests that they form part of a chain where their orientation, determined by the hybridization of the neighbour carbon atom, is favourable for the interaction of light with the IR active components of both (symmetric and asymmetric) dipole moments.

The gain band at 2343 cm^{-1} in Fig. 8 is due to CO_2 , produced at 1.50 V. This product slowly diffuses out of the thin solution layer between the electrode and IR window, and can therefore be detected although the sample spectrum was taken after turning the potential back to 0.35 V.

As shown by DEMS, strongly adsorbed species of propanol can be reduced at potentials in the H-atom electroadsorption region. The nature of the species remaining on the electrode can be established by FTIR using the experimental program insert of Fig. 8(b). Accordingly, after adsorption, a reduction step down to 0.05 V was applied. Then, the potential was set back to 0.35 V and the reference spectrum was taken. Subsequently, an oxidation step to 1.3 V was applied in order to oxidize the remaining residues. Finally, the potential was set back to 0.35 V and the sample spectrum was measured.

The spectrum in Fig. 8(b) shows no remaining adsorbates containing C–H bonds. In contrast, the CO band intensity grows in comparison to the experiment without the reduction step, spectrum (a), suggesting that at least a fraction of the initial adsorbates formed from $n\text{-PrOH}$ are oxygenated species other than CO. These species are cleaved at 0.05 V losing a hydrocarbon part and leaving CO adsorbed on the metal. The increase in the intensity of the CO band after this procedure is about 28%.

In a series of experiments $n\text{-PrOH}$ was introduced in the cell while the working electrode was held at 0.05 V in the base electrolyte. At this potential propanol is not significantly adsorbed [10]. Reference spectra were taken at 0.05 V and sample spectra at 0.22 V during the adsorption of propanol. Under these conditions we observed a band at 1510 cm^{-1} , which can be assigned to the C=O stretching vibration of an acyl adsorbate [33] (see Fig. 9). The positive-going band at 1464

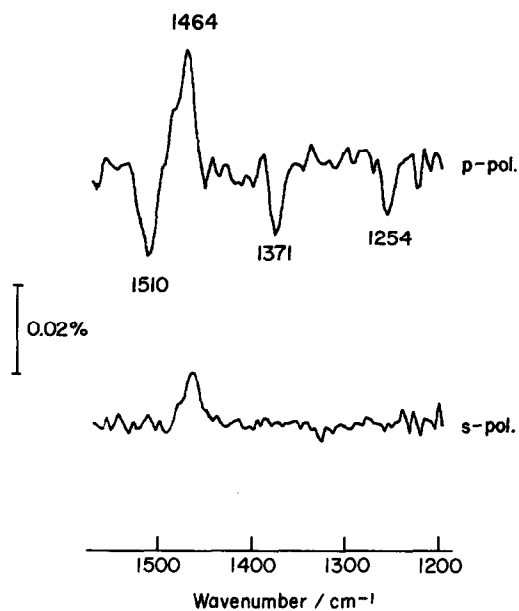


Fig. 9. FTIR reflectance spectra with s- and p-polarized radiation during the adsorption of *n*-PrOH at 0.22 V (1000 scans, 8 cm^{-1} resolution). Propanol was introduced in the cell at 0.05 V and the reference spectrum was taken at this potential (propanol is not adsorbed under these conditions).

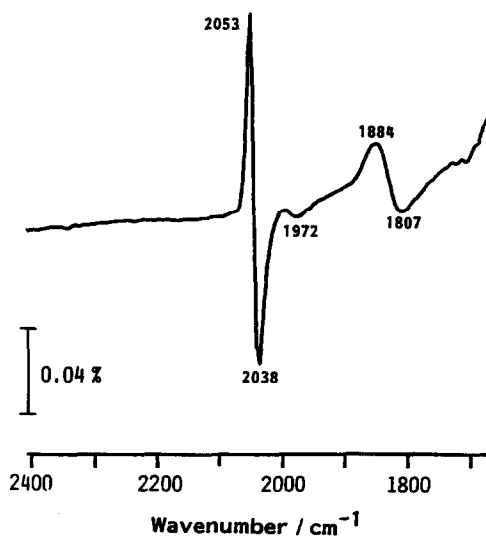


Fig. 10. FTIR reflectance spectra taken alternating the potential between 0.225 V and 0.350 V. 30000 interferograms were collected at each potential. The potential was changed every 1000 scans.

cm^{-1} is due to the CH_3 deformation of propanol being consumed in the solution (we see this band also in the spectrum taken with s-polarized radiation). The other gain bands in the spectrum with p-polarized radiation were not identified. CH groups present deformation and rocking bands in this region and the C–O stretching of alcohol structures is expected around 1200 cm^{-1} [34].

Finally, FTIR spectra were obtained by applying a potential modulation between 0.35 and 0.22 V, i.e. the potential range where no soluble products can be formed (Fig. 10). We observed no bands in the $2800\text{--}3000 \text{ cm}^{-1}$ range. The band shift with the potential is probably very small and the signals cancel out in the difference spectrum. Potential modulation also produces a redistribution of CO adsorbates on Pt. Therefore, under these conditions, three differently coordinated CO adsorbates can be observed: linear CO (strong bipolar band at $2053\text{--}2038 \text{ cm}^{-1}$); double-bonded CO (weak band at 1972 cm^{-1}); and triple bonded CO (medium bipolar band at $1884\text{--}1807 \text{ cm}^{-1}$). These assignments are in agreement with data already reported in the literature for CO adsorbed on Pt and other metals in UHV [35], or in aqueous solutions of methanol [36] and other organic compounds [37].

DISCUSSION

Summary of experimental findings

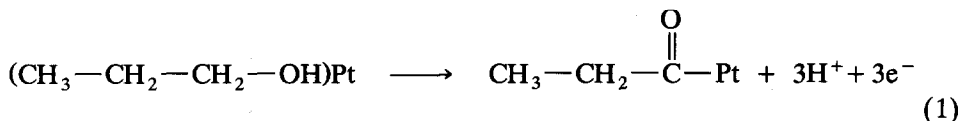
1. In the presence of propanol in the bulk, oxidation to propanal starts before 0.40 V (Fig. 1). Above 0.70 V propionic acid is observed as soluble product (Figs. 5 and 7). Below 0.20 V ethane, propane and methane are formed (Figs. 2 and 4).
2. CO_2 is the only oxidation product from the strongly adsorbed residues of *n*-PrOH (Fig. 3).
3. A part of the strongly bonded residues requires more than one potential cycle to be oxidized completely (Fig. 3(b)).
4. Adsorbed CO and species containing CH_3 and CH_2 are the strongly adsorbed residues of propanol on platinum (Fig. 8).
5. After cycling the potential in the hydrogen region, the hydrocarbon chain of *n*-PrOH adsorbate is lost and adsorbed CO remains as an adsorbed residue (Fig. 8).
6. Combining point 5 with the results of DEMS (Fig. 3), which show an increase of E_{p1} and a decrease of E_{p2} after cycling the potential in the H-region, we conclude that the species reacting under E_{p1} is adsorbed carbon monoxide while under peak E_{p2} oxidation of the hydrocarbon chain occurs.

A reaction scheme for *n*-PrOH must explain these observations.

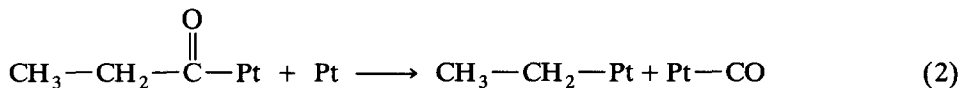
Reactions forming adsorbed species

The initial interaction of *n*-PrOH with a Pt surface could be a weak adsorption involving an excess of *n*-PrOH molecules in the double layer [$(\text{CH}_3\text{--CH}_2\text{CH}_2\text{--OH})\text{Pt}$]. A sequence of steps including dehydrogenation of the $\text{C}\alpha$ atom and of the

OH group could then produce the adsorbed acyl radical observed in the spectrum of Fig. 9:



As long as free Pt sites are available at the adsorption potential, the acyl adsorbate can react further to adsorbed CO and ethyl adsorbates:



The reaction can proceed further at more positive potentials as CO starts being oxidized, but due to the increasing coverage with oxide at potentials above 0.70 V some of the remaining acyl adsorbate can remain unoxidized. In a cyclic potential scan the remaining acyl adsorbate can dissociate according to (2), as the Pt oxide is reduced, thus causing the peak E_{p3} observed during the negative scan.

At 0.05 V the acyl radical can interact with adsorbed hydrogen to form ethane, leaving adsorbed CO.

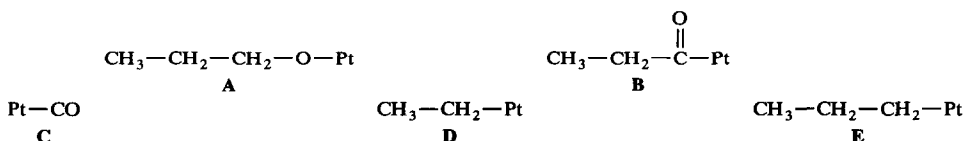
Although we have no evidence for other adsorbed species, weakly adsorbed reaction intermediates which do not survive the exchange of electrolyte should also be formed. It has been shown that the first step during the adsorption of alcohols in UHV experiments is abstraction of the hydrogen atom from the OH-group [38]. An alkoxy intermediate is thus formed. The stability of adsorbed alkoxy radicals from different alcohols depends on the nature of the metal substrate and the temperature [33,38]. The characteristic $\nu(\text{CO})$ frequency for adsorbed alkoxy radicals on different metals lies at ca. 1000 cm^{-1} . In IR spectra obtained in the presence of propanol this frequency is overlapped with the 1004 cm^{-1} feature of the alcohol. We were therefore unable to observe the characteristic propoxy band. As a working hypothesis which still has to be confirmed, we suggest that during the adsorption process of *n*-PrOH parallel to reaction (1) a propoxy radical is formed, which results from the abstraction of a hydrogen atom from the OH-group:



If the adsorption takes place in the hydrogen region, the C-O bond breaks, oxygen reacts with adsorbed hydrogen, and a propyl radical is formed:



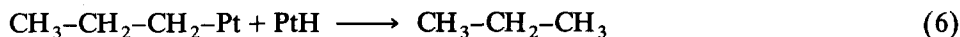
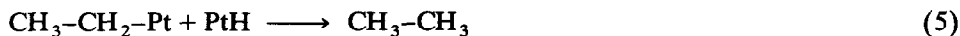
Summarizing the results of reactions (1-4) we suggest that following species are formed during the adsorption of *n*-PrOH on platinum:



From these, species B-E constitute the strongly adsorbed residues of *n*-PrOH.

*Reactions producing soluble products**Hydrocarbons*

Below 0.2 V **D** and **E** can be reduced to ethane and propane:

*Carbon dioxide*

From the oxidation products, CO_2 is produced only through the oxidation of the strongly adsorbed intermediates **B-E**.

1. Providing that free Pt sites are available, the acyl adsorbate **B** must first dissociate according to reaction (2), producing adsorbates **C** and **D**.
2. Adsorbed CO **C** is oxidized under E_{p1} and E_{p3} .
3. It is not known to what extent ethyl and propyl adsorbates (**D** and **E**) should break before they can be oxidized under E_{p2} . Since the cracking requires free Pt places, the complete oxidation may require several potential cycles.

Propanal and propionic acid

Propanal was observed only in the presence of propanol in the solution. The fact that propanal is already formed at 0.40 V suggests that the reactive intermediate is an oxygen-containing species which only needs to lose one hydrogen atom in order to form the aldehyde, see eqn. 3. The aldehyde molecule can desorb or react to propionic acid in the presence of PtOH (at ca. 0.7 V, Fig. 5):



All these reactions are summarized in the general arrangement (Scheme 1) for the reactions of *n*-PrOH on Pt.

CONCLUDING REMARKS

The results presented and discussed here, based on the spectroscopical investigation of the reaction, give a realistic picture of the processes occurring during *n*-PrOH adsorption, reduction and oxidation on platinum.

The results of DEMS and in situ FTIR can be reasonably interpreted through the general scheme for the reactions discussed above. Although the propoxy adsorbate could not be definitely demonstrated, its presence can explain several experimental features. Propanal and propionic acid must be formed through a species which is not as stable as the acyl adsorbate.

The adsorption of *n*-PrOH to Pt through $\text{C}\alpha$ weakens the bond between $\text{C}\alpha$ and its neighbouring C atom. This will assist acyl radical dissociation into CO and ethyl adsorbate. But adsorption of *n*-PrOH through the oxygen should avoid the weakening of the C1-C2 bond. Therefore, a parallel path involving the propoxy radical must result in C_3 intermediates or products as proposed above.

ACKNOWLEDGEMENTS

We thank the Gobierno de Canarias (Spain) for a fellowship to E.P.. Financial support from the Deutsche Forschungsgemeinschaft (DFG) is gratefully acknowledged.

REFERENCES

- 1 B.B. Damaskin, O.A. Petrii and V.V. Batrakov, Adsorption of Organic Compounds on Electrodes, Plenum, New York, 1971, p. 335.
- 2 M.W. Breiter, in J.O'M. Bockris and B.E. Conway (Eds.), Modern Aspects of Electrochemistry, Vol. 10, Plenum, New York, 1975, p. 161.
- 3 G. Horányi, *Electrochim. Acta*, 31 (1986) 1095.
- 4 O.A. Petrii, B.I. Podlovchenko, A.N. Frumkin and Hira Lal, *J. Electroanal. Chem.*, 10 (1965) 253.
- 5 R.S. Gonçalves, J.M. Léger and C. Lamy, *Electrochim. Acta*, 33 (1988) 1581.
- 6 V.S. Bagotzkii, Yu.B. Vassiliev and O.A. Khazova, *J. Electroanal. Chem.*, 81 (1977) 229.
- 7 M.C. Arévalo, E. Pastor, S. González and A.J. Arvia, *Electrochim. Acta*, 36 (1991) 2183.
- 8 M.C. Arévalo, C. Gomis-Bas, E. Pastor, S. González and A.J. Arvia, *Electrochim. Acta*, 37 (1992) 1083.
- 9 M.C. Arévalo, E. Pastor, S. González, A. Arévalo, M.C. Giordano and A.J. Arvia, *J. Electroanal. Chem.*, 281 (1990) 245.
- 10 E. Pastor, M.C. Arévalo, S. González and A.J. Arvia, *Electrochim. Acta*, 36 (1991) 2003.
- 11 A.B. Delgado, A.M. Castro Luna, W.E. Triaca and A.J. Arvia, *J. Electrochem. Soc.*, 129 (1982) 1493.
- 12 R.S. Gonçalves, J.M. Léger and C. Lamy, *Electrochim. Acta*, 34 (1989) 433.
- 13 C.S. Fugivara, P.T.A. Sumodjo and T. Rabockai, *Electrochim. Acta*, 34 (1989) 363.
- 14 O. Wolter and J. Heitbaum, *Ber. Bunsenges. Phys. Chem.*, 88 (1984) 6.
- 15 B. Bittins-Cattaneo, E. Cattaneo, P. Königshoven and W. Vielstich, in A.J. Bard (Ed.), *Electroanalytical Chemistry: A Series of Advances*, Vol. 17, Marcel Dekker, 1991, p. 181.
- 16 A. Bewick and S. Pons, in R.J.H. Clark and R.E. Hester (Eds.), *Advances in Infrared and Raman Spectroscopy*, Vol. 12, W. Heyden, London, 1985, Ch. 1.
- 17 K. Foley and S. Pons, *Anal. Chem.*, 57 (1985) 945.
- 18 T. Iwasita and F.C. Nart, *J. Electroanal. Chem.*, 295 (1990) 215.
- 19 M.V. Christov and E.I. Sokolova, *J. Electroanal. Chem.*, 175 (1984) 183.
- 20 I. Podlovchenko, O.A. Petrii, A.N. Frumkin and Hira Lal, *J. Electroanal. Chem.*, 11 (1966) 12.
- 21 Th. Hartung, Ph.D. Thesis, Witten/Herdecke University (1989).
- 22 S.G. Sun, D.F. Yang and Z.W. Tian, *J. Electroanal. Chem.*, 289 (1990) 177.
- 23 P. Stonehart and C. Kohlmayr, *Electrochim. Acta*, 17 (1972) 369.
- 24 T. Iwasita, W. Vielstich and E. Santos, *J. Electroanal. Chem.*, 229 (1987) 367.
- 25 F.C. Nart, H. Polligkeit and T. Iwasita, *Ber. Bunsenges. Phys. Chem.*, 95 (1991) 638.
- 26 E. Stenhagen, S. Abrahamsson and F.W. McLafferty (Eds.), *Atlas of Mass Spectral Data*, Interscience Publishers, New York, 1969.
- 27 F.C. Nart and T. Iwasita, *J. Electroanal. Chem.*, 322 (1992) 289.
- 28 N.A. Balaschova, *Z. Phys. Chem. (Leipzig)*, 207 (1957) 340.
- 29 A. Wieckowski, P. Zelenay and K. Varga, *J. Chim.*, 88 (1991) 1247.
- 30 L.H. Little, *Infrared Spectra of Adsorbed Species*, Academic Press, London, 1966.
- 31 S.A. Francis, *J. Chem. Phys.*, 18 (1950) 861.
- 32 G. Blyholder and L.D. Neff, *J. Catal.*, 2 (1963) 138.
- 33 J.L. Davis and M.A. Barteau, *Surf. Sci.*, 235 (1990) 235.
- 34 G. Sócrates, *Infrared Characteristic Group Frequencies*, John Wiley, 1980.

- 35 N. Sheppard and T.T. Nguyen, in R.H.H. Clark and R.E. Hester (Eds.), *Advances in Infrared and Raman Spectroscopy*, Vol. 5, Heyden, London, 1978, p. 67.
- 36 F.C. Nart and T. Iwasita, *J. Electroanal. Chem.*, 317 (1991) 291.
- 37 T. Iwasita, F.C. Nart, W. Vielstich and B. López, *Electrochim. Acta*, 37 (1992) 2361.
- 38 B.A. Sexton, *Surf. Sci.*, 88 (1979) 299.